Proc. of JSCE,
No. 194, Oct. 1971

ELASTO-PLASTIC ANALYSIS OF STEEL STRUCTURES CONSIDERING THE EFFECTS OF RESIDUAL STRESS AND FINITE DEFORMATION

By Toshiaki OHTA and Tokuya YAMASAKI***

ABSTRACT

A general beam theory is developed capable of treating elasto-plastic bending behavior of steel structures subjected to (a) incrementary load and (b) repeated load combined with axial load; Attention is focused on the evaluation of the effects of residual stress and finite deformation.

Extended complementary energy method is employed throughout the analysis and numerical results are presented for stress, curvature and deflection of steel members with rectangular and I-sections of the structures.

Problems of plastic stability are also considered theoretically from the same energy viewpoint.

1. INTRODUCTION

The classical approach[1),2),3),4),5)] to the evaluation of inelastic behavior of steel member is generally based on the moment-curvature equation.

In this case, however, when a steel member having residual stress is subjected to variable cyclic load combined with axial load, serious difficulty is encountered in formulating exact representations[2)] for the inelastic behavior. For clarity, function of the moment-curvature equation changes extremely its form under the above mentioned load condition, and the analytical procedure due to such function can thus be much complicated.

The resolution of the foregoing difficulty may be given by using the extended complementary energy method of continuum mechanics together with the generalized moment-curvature formula which will be derived in this paper by the authors.

This can be accomplished by estimating directly the stress-strain relation for the given loads based on the numerical integration technique[6),7),8),9)] and trial and error method.

As a result, the cumbersome but otherwise rigorous solution of the elasto-plastic beam theory is replaced herein by much simpler generalized one with sufficient engineering accuracy. And the inelastic bending problems for steel structures with residual stress, subjected to combined loads such as combined bending moment and axial force, are solved by the numerical analysis and results are presented for the stress, the moment-curvature relation, the deflection and so on.

It is also shown that the elasto-plastic finite deformations of structures can be easily analyzed by the extended complementary energy method[8)].

Furthermore, in this investigation, problems of plastic stability, usually accompanied with the bending problems above mentioned, are considered by using matrix analysis from the same energy viewpoint.

2. ASSUMPTIONS

The method considered herein makes the following assumptions.

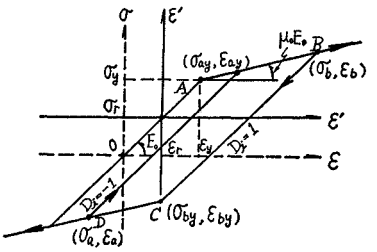

Fig. 1 Stress-Strain Diagram.

1) The stress-strain history curve for steel is idealized as shown in Fig. 1.
2) The plane sections of the member remain plane during bending.
3) The member is of uniform section.

* Assistant Professor, Department of Civil Engineering, Faculty of Engineering, Miyazaki University
** Assistant General Manager, Steel Structural Research Laboratories, KAWASAKI STEEL Coorporation

4) The member is subjected to bending moment and axial force.
5) Effect of shearing stress is neglected.
6) Possibility of local buckling is disregarded.

The coordinate systems are as follows: The coodinate x is parallel to the axis of the member and y is perpendiculer to the neutral plane.

3. ELASTO-PLASTIC BENDING

(1) Strees-Strain Relation

Denoting normal stress and strain in x direction by σ and ε, respectively, the stress-strain relation for the steel, as shown in Fig. 1, is generally expressed by the following non-dimensional from.

$$\bar{\sigma}=\nu(\bar{\varepsilon}-\bar{\varepsilon}^*) \quad \cdots\cdots(1)$$

where $\bar{\sigma}=\sigma/\sigma_y$, $\bar{\varepsilon}=\varepsilon/\varepsilon_y$, $\bar{\varepsilon}^*=\varepsilon^*/\varepsilon_y$

σ_y : yield stress of steel,

ε_y : yield strain of steel.

Table 1 Values of σ_a, ε_a, $\cdots\sigma_{by}$, ε_{by} and D_i.

Step 1	$\sigma_{ay}=\varepsilon_{ay}-\varepsilon_a'+\sigma_a'$ $\varepsilon_a=\varepsilon_a'$ $\varepsilon_{ay}=\varepsilon_{ay}'$ $\varepsilon_b=\varepsilon_b'$ $\varepsilon_{by}=\varepsilon_{by}'$ $\sigma_a=\sigma_a'$ $\sigma_b=\sigma_b'$ $\sigma_{by}=\sigma_{by}'$ $D_i=D_i'$
Step 2	$\varepsilon_b=\varepsilon$ $\varepsilon_{by}=\varepsilon_b'-2\varepsilon_y$ $\varepsilon_a=\varepsilon_{by}$ $\sigma_b=\mu_0F_0(\varepsilon_b-\varepsilon_{ay}')+\sigma_{ay}'$ $\varepsilon_{ay}=\varepsilon_{ay}'$ $\sigma_a=\sigma_a'$ $\sigma_{ay}=\sigma_{ay}'$ $D_i=1$
Step 3	$\sigma_{by}=\sigma_{by}'-\varepsilon_b'+\sigma_b'$ $\varepsilon_a=\varepsilon_a'$ $\varepsilon_{ay}=\varepsilon_{ay}'$ $\varepsilon_b=\varepsilon_b'$ $\varepsilon_{by}=\varepsilon_{by}'$ $\sigma_a=\sigma_a'$ $\sigma_{ay}=\sigma_{ay}'$ $\sigma_b=\sigma_b'$ $D_i=D_i'$
Step 4	$\varepsilon_a=\varepsilon$ $\varepsilon_{ay}=\varepsilon_a'+2\varepsilon_y$ $\varepsilon_b=\varepsilon_{ay}$ $\sigma_a=\mu_0F_0(\varepsilon_a-\varepsilon_{by}')+\sigma_{by}'$ $\varepsilon_{by}=\varepsilon_{by}'$ $\sigma_b=\sigma_b'$ $\sigma_{by}=\sigma_{by}'$ $D_i=-1$

Because the procedure is programmed for an electronic computer such that the initial values of ε_a, ε_{ay}, $\cdots$ σ_{by} are given by Eq. (2), the values of ν, ε^* and ε_a, ε_{ay}, $\cdots$for the given load are taken as follows;

If $\varepsilon_a<\varepsilon<\varepsilon_{ay}$ and $D_i=-1$ then $\nu=1$, $\varepsilon^*=\varepsilon_a-\sigma_a/E_0$ and ε_a, ε_{ay}, $\cdots$are defined as shown at rank of Step 1 (loading at the elastic state) in Table 1.

If $\varepsilon\geq\varepsilon_b$ then $\nu=\mu_0$, $\varepsilon^*=\varepsilon_{ay}-\sigma_{ay}/\mu_0E_0$ and ε_a, ε_{ay}, $\cdots$are defined as shown at rank of Step 2 (loading at the elasto-plastic state).

If $\varepsilon_{by}<\varepsilon<\varepsilon_b$ and $D_i=1$ then $\nu=1$, $\varepsilon^*=\varepsilon_b-\sigma_b/E_0$ and ε_a, ε_{ay}, $\cdots$are defined at rank of Step 3 (unloading elastic state).

If $\varepsilon\leq\varepsilon_a$ then $\nu=\mu_0$, $\varepsilon^*=\varepsilon_{by}-\sigma_{by}/\mu_0E_0$ and ε_a, ε_{ay}, $\cdots$are defined at rank of Step 4 (unloading at the elasto-plastic state).

In Table 1, values of ε_a', ε'_{ay}, $\cdots$ D'_i are the ones of ε_a, ε_{ay},$\cdots D_i$, at the former load-step, respectively.

While, the initial values of ε_a, ε_{ay}, $\cdots$are given as.

$$\left.\begin{aligned}&\sigma_a=\sigma_{by}=-\sigma_y-\sigma_r,\ \sigma_b=\sigma_{ay}=\sigma_y-\sigma_r,\ D_i=-1,\\&\varepsilon_a=\varepsilon_{by}=-\varepsilon_y-\varepsilon_r,\ \varepsilon_b=\varepsilon_{ay}=\varepsilon_y-\varepsilon_r,\end{aligned}\right\}$$
$$\cdots\cdots(2)$$

where σ_r, ε_r : residual stress and strain, respectively, $(\sigma_{ay}, \varepsilon_{ay})$, $(\sigma_b, \varepsilon_b)$, $(\sigma_{by}, \varepsilon_{by})$, $(\sigma_a, \varepsilon_a)$: stresses and strains at the points A, B, C and D in Fig. 1, respectively.

Consider the member section shown in Fig. 2; Relationships between strains and therefore stresses at the various depth of k (k=1, 2$\cdots$) can be derived from the geometry of strain distribution.

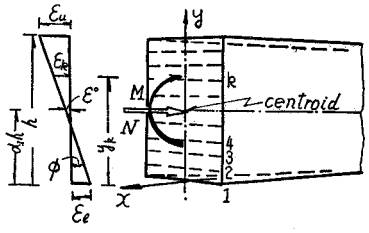

Fig. 2 Strain-Distribution Diagram for Rectangular Section.

$$\bar{\varepsilon}=[(1-\bar{y}_k)\ \bar{y}_k]\begin{bmatrix}\bar{\varepsilon}_l\\ \bar{\varepsilon}_u\end{bmatrix},\ (k=1,\ 2,\ \cdots)\quad\cdots\cdots(3)$$

where $\bar{y}_k=y_k/h$, $\bar{\varepsilon}_l=\varepsilon_l/\varepsilon_y$, $\bar{\varepsilon}_u=\varepsilon_u/\varepsilon_y$,

ε_k : strain at level k,

ε_u, ε_l : upper and lower extreme fiber strains, respectively,

y_k : depth of level k,

h : depth of cross section.

From Eqs. (1) and (3), stress at level k of the member is expressed as follows;

$$\bar{\sigma}_k=[\nu_k(1-\bar{y}_k)\ \nu_k\bar{y}_k]\begin{bmatrix}\bar{\varepsilon}_l\\ \bar{\varepsilon}_u\end{bmatrix}-\nu_k\bar{\varepsilon}_k^*\quad\cdots\cdots(4)$$

(2) General Formula for the Moment-Curvature Relations

For equilibrium, external forces must equall to internal forces.

Therefore,

$$\begin{bmatrix}0 & 1\\ 1 & -\alpha_1h\end{bmatrix}\begin{bmatrix}M\\ N\end{bmatrix}=\begin{bmatrix}\int\sigma\,dA_0\\ -\int\sigma y\,dA_0\end{bmatrix}\quad\cdots\cdots(5)$$

where M : external bending moment,

N : external axial force,

dA_0 : elementary area of cross section,

α_1h : depth of centroid of cross section.

Substituting Eq. (4) into Eq. (5) and replacing M, N by $\bar{M}$ ($=M/M_y$), $\bar{N}$ ($=N/N_y$), Eq. (5) will become

$$\begin{bmatrix}0 & 1\\ 1 & -\alpha_1\alpha_0\end{bmatrix}\begin{bmatrix}\bar{M}\\ \bar{N}\end{bmatrix}$$

$$= \begin{bmatrix} \int \nu(1-\bar{y})\frac{dA_0}{A_0} & \int \nu\,\bar{y}\frac{dA_0}{A_0} \\ \alpha_0\int \nu(1-\bar{y})\bar{y}\frac{dA_0}{A_0} & \alpha_0\int \nu\bar{y}^2\frac{dA_0}{A_0} \end{bmatrix} \begin{bmatrix} \bar{\varepsilon}_l, \\ \bar{\varepsilon}_u \end{bmatrix} - \begin{bmatrix} \int \nu\bar{\varepsilon}^*\frac{dA_0}{A_0} \\ \alpha_0\int \nu\,\bar{y}\,\bar{\varepsilon}^*\frac{dA_0}{A_0} \end{bmatrix} \quad \cdots\cdots(6)$$

where $M_y=E_0 I\phi_y$: yield moment, $N_y=\sigma_y A_0$,
$\alpha_0=N_y h/M_y$,
A_0 : cross sectional area,
E_0 : modulus of elasticity,
I : moment of inertia of cross section,
ϕ_y : yield curvature.

On the other hand, curvature ϕ and strain ε^0 at the centroid of cross section are given as follows (See Fig. 2);

$$\begin{bmatrix} \bar{\phi} \\ \bar{\varepsilon}^0 \end{bmatrix} = \begin{bmatrix} \phi/\phi_y \\ \varepsilon^0/\varepsilon_y \end{bmatrix} = \begin{bmatrix} \alpha_2 & -\alpha_2 \\ 1-\alpha_1 & \alpha_1 \end{bmatrix} \begin{bmatrix} \bar{\varepsilon}_l \\ \bar{\varepsilon}_u \end{bmatrix} \quad \cdots\cdots(7)$$

From Eqs. (6) and (7), we find the required equation as,

$$\begin{bmatrix} \bar{\phi} \\ \bar{\varepsilon}^0 \end{bmatrix} = \begin{bmatrix} F_{11} & F_{12} \\ F_{21} & F_{22} \end{bmatrix} \begin{bmatrix} \bar{M} \\ \bar{N} \end{bmatrix} + \begin{bmatrix} G_1 \\ G_2 \end{bmatrix} \quad \cdots\cdots(8)$$

where

$$\begin{bmatrix} F_{11} & F_{12} \\ F_{21} & F_{22} \end{bmatrix} = \begin{bmatrix} \alpha_2 & -\alpha_2 \\ 1-\alpha_1 & \alpha_1 \end{bmatrix} \begin{bmatrix} \boldsymbol{D}_0 \end{bmatrix}^{-1} \begin{bmatrix} 0 & 1 \\ 1 & -\alpha_1\alpha_0 \end{bmatrix}$$

$$\begin{bmatrix} \boldsymbol{D}_0 \end{bmatrix} = \begin{bmatrix} \int \nu(1-\bar{y})\frac{dA_0}{A_0} & \int \nu\,\bar{y}\frac{dA_0}{A_0} \\ \alpha_0\int \nu(1-\bar{y})\bar{y}\frac{dA_0}{A_0} & \alpha_0\int \nu\bar{y}^2\frac{dA_0}{A_0} \end{bmatrix}$$

$$\begin{bmatrix} G_1 \\ G_2 \end{bmatrix} = \begin{bmatrix} \alpha_2 & -\alpha_2 \\ 1-\alpha_1 & \alpha_1 \end{bmatrix} \begin{bmatrix} \boldsymbol{D}_0 \end{bmatrix}^{-1} \begin{bmatrix} \boldsymbol{E}_0 \end{bmatrix}$$

$$\begin{bmatrix} \boldsymbol{E}_0 \end{bmatrix} = \begin{bmatrix} \int \nu\bar{\varepsilon}^*\frac{dA_0}{A_0} \\ \alpha_0\int \nu\bar{\varepsilon}^*\bar{y}\frac{dA_0}{A_0} \end{bmatrix}, \quad \alpha_2 = \frac{r\varepsilon_y}{h\phi_y}$$

a) Rectangular Section

Let consider a rectangular section shown in Fig. 3 as the first example, elements $\boldsymbol{D}_{ij}$ and $\boldsymbol{E}_{ij}(i, j=1, 2)$ of matrices $[\boldsymbol{D}_0]$ and $[\boldsymbol{E}_0]$ in question are obtained by using so called Trapezoidal formula as,

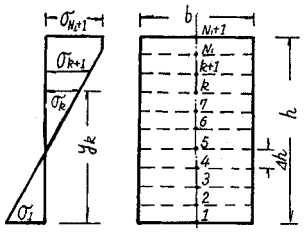

Fig. 3 Stress-Distribution Diagram for Rectangular Section.

$$\boldsymbol{D}_{11}=\Delta\bar{h}\sum_{k=1}^{N_1}\{\nu_k(1-\bar{y}_k)+\nu_{k+1}(1-\bar{y}_{k+1})\}/2,$$

$$\boldsymbol{D}_{12}=\Delta\bar{h}\sum_{k=1}^{N_1}\{\nu_k\bar{y}_k+\nu_{k+1}\bar{y}_{k+1}\}/2,$$

$$\boldsymbol{D}_{21}=\alpha_0\Delta\bar{h}\sum_{k=1}^{N_1}\{(3\bar{y}_k+\Delta\bar{h})(1-\bar{y}_k)\nu_k + (3\bar{y}_k+2\Delta\bar{h})(1-\bar{y}_{k+1})\nu_{k+1}\}/6,$$

$$\boldsymbol{D}_{22}=\alpha_0\Delta\bar{h}\sum_{k=1}^{N_1}\{(3\bar{y}_k+\Delta\bar{h})\bar{y}_k\nu_k + (3\bar{y}_k+2\Delta\bar{h})\bar{y}_{k+1}\nu_{k+1}\}/6,$$

$$\boldsymbol{E}_{11}=\Delta\bar{h}\sum_{k=1}^{N_1}\{\nu_k\bar{\varepsilon}_k^*+\nu_{k+1}\bar{\varepsilon}_{k+1}^*\}/2$$

$$\boldsymbol{E}_{21}=\alpha_0\Delta\bar{h}\sum_{k=1}^{N_1}\{(3\bar{y}_k+\Delta\bar{h})\nu_k\bar{\varepsilon}_k^* + (3\bar{y}_k+2\Delta\bar{h})\nu_{k+1}\bar{\varepsilon}_{k+1}^*\}/6,$$

where $\Delta\bar{h}=\Delta h/h$,

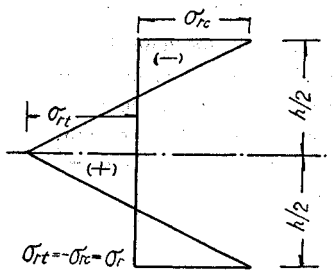

Fig. 4 Residual Stress-Distribution Diagram for Rectangular Section.

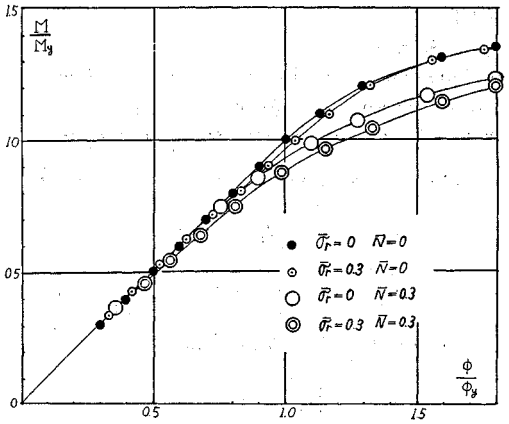

Fig. 5 Moment-Curvature Relation for Rectangular Section under Incrementary Loading.

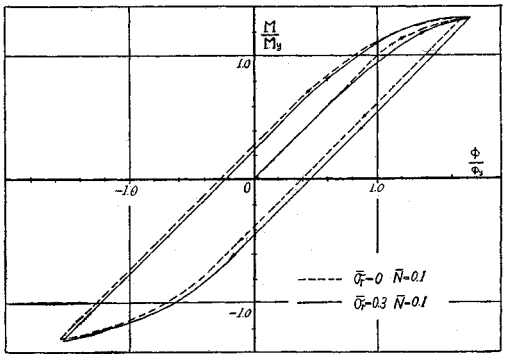

Fig. 6 Moment-Curvature Relation for Rectangular Section under Cycric Loading.

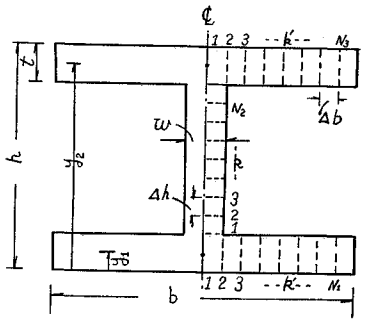

Fig. 7 I-Section.

Δh : length of the divided element.

From the above result, moment-curvature relations are obtained for the rectangular section[2] with residual stress of Fig. 4 by running computer program with $\Delta h=h/10$, $\sigma_{rt}=-\sigma_{rc}=0.3\,\sigma_y$, $\sigma_y=2\,100$ kg/cm², $E_0=2.1\times10^6$ kg/cm², $\mu_0=0.005$ and $\bar{N}$ having the values 0 and 0.3, respectively, and plotted in Fig. 5.

On the other hand, moment-curvature hysteresis curve of the same section can be given as in Fig. 6 under cyclic bending combined with axial force $\bar{N}=0.1$.

b) I-Section

A wide-flange I-section shown in Fig. 7 is considered as the second illustrative example.

In this case, the elements $\boldsymbol{D}_{ij}$ and $\boldsymbol{E}_{ij}$ are

$$\begin{aligned}\boldsymbol{D}_{11}=w\Delta h\Big[&\sum_{k=1}^{N_2}\{\nu_k(1-\bar{y}_k)+\nu_{k+1}(1-\bar{y}_{k+1})\}\\&+2t\Delta b\Big\{\sum_{k'=1}^{N_3}\bar{y}_1(\nu_{k'}+\nu_{k'+1})\\&+\sum_{k'=1}^{N_1}\bar{y}_2(\nu_{k'}+\nu_{k'+1})\Big\}\Big/w\Delta h\Big]\Big/2A_0,\\ \boldsymbol{D}_{12}=w\Delta h\Big[&\sum_{k=1}^{N_2}(\nu_k\bar{y}_k+\nu_{k+1}\bar{y}_{k+1})\\&+2t\Delta b\Big\{\sum_{k'=1}^{N_3}\bar{y}_2(\nu_{k'}+\nu_{k'+1})\\&+\sum_{k'=1}^{N_1}\bar{y}_1(\nu_{k'}+\nu_{k'+1})\Big\}\Big/w\Delta h\Big]\Big/2A_0,\\ \boldsymbol{D}_{21}=\alpha_0 w\Delta h\Big[&\sum_{k=1}^{N_2}\{\nu_k(3\bar{y}_k+\Delta\bar{h})(1-\bar{y}_k)\\&+\nu_{k+1}(3\bar{y}_k+2\Delta\bar{h})(1-\bar{y}_{k+1})\}\\&+6t\Delta b\Big\{\sum_{k'=1}^{N_3}\bar{y}_1\bar{y}_2(\nu_{k'}+\nu_{k'+1})\\&+\sum_{k'=1}^{N_1}\bar{y}_1\bar{y}_2(\nu_{k'}+\nu_{k'+1})\Big\}\Big/w\Delta h\Big]\Big/6A_0,\\ \boldsymbol{D}_{22}=\alpha_0 w\Delta h\Big[&\sum_{k=1}^{N_2}\{\nu_k(3\bar{y}_k+\Delta\bar{h})\bar{y}_k\\&+\nu_{k+1}(3\bar{y}_k+2\Delta\bar{h})\bar{y}_{k+1}\}\\&+6t\Delta b\Big\{\sum_{k'=1}^{N_3}\bar{y}_1^{\,2}(\nu_{k'}+\nu_{k'+1})\\&+\sum_{k'=1}^{N_1}\bar{y}_2^{\,2}(\nu_{k'}+\nu_{k'+1})\Big\}\Big/w\Delta h\Big]\Big/6A_0,\\ \boldsymbol{E}_{11}=w\Delta h\Big[&\sum_{k=1}^{N_2}\{\nu_k\bar{\varepsilon}_k{}^*+\nu_{k+1}\bar{\varepsilon}_{k+1}{}^*\}\\&+2t\Delta b\Big\{\sum_{k'=1}^{N_3}(\nu_{k'}\bar{\varepsilon}_{k'}{}^*+\nu_{k'+1}\bar{\varepsilon}_{k'+1}{}^*)\\&+\sum_{k'=1}^{N_1}(\nu_{k'}\bar{\varepsilon}_{k'+1}{}^*+\nu_{k'+1}\bar{\varepsilon}_{k'+1}{}^*)\Big\}\Big/\\&w\Delta h\Big]\Big/2A_0,\\ \boldsymbol{E}_{21}=w\Delta h\Big[&\sum_{k=1}^{N_2}\{\nu_k(3\bar{y}+\Delta\bar{h})\bar{\varepsilon}_k{}^*\\&+\nu_{k+1}(3\bar{y}_k+2\Delta\bar{h})\bar{\varepsilon}_{k+1}{}^*\}\\&+6t\Delta b\Big\{\sum_{k'=1}^{N_3}\bar{y}_2(\nu_{k'}\bar{\varepsilon}_{k'}{}^*+\nu_{k'+1}\bar{\varepsilon}_{k'+1}{}^*)\\&+\sum_{k'=1}^{N_1}\bar{y}_1(\nu_{k'}\bar{\varepsilon}_{k'}+\nu_{k'+1}\bar{\varepsilon}_{k'+1}{}^*)\Big\}\Big/\\&w\Delta h\Big]\Big/6A_0,\end{aligned}$$

where w : width of web,

y_1, y_2 : depth of the centroid of lower and upper flanges, respectively,

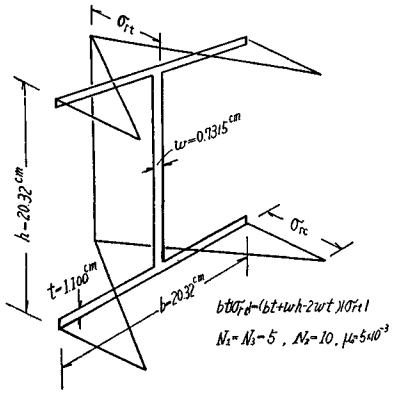

Fig. 8 Residual Stress-Distribution Diagram for I-Section.

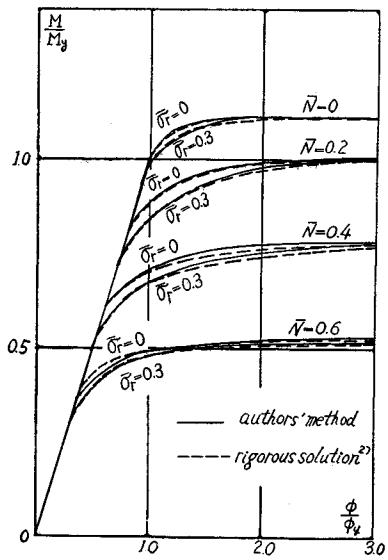

Fig. 9 Moment-Curvature Relation for I-Section (Strong Axis) under Incrementary Loading.

h : depth of cross section,
t : thickness of flange,
b : width of flange,
Δb : elemental length of b,
Δh : elemental length of h,
A_0 : total cross-sectional area,
k' : number of element in flange, used as suffix,
k : number of element in web, used as suffix.

From the result obtained above, the moment-curvature relation for I-section[2] of Fig. 8, named 8 WF Section ($\sigma_y=2\,812$ kg/cm^2, $E_0=2.1\times10^6$ kg/cm^2), will be obtained as in Fig. 9.

Good agreement is obtained between the result of this method and rigorous solution[2].

(3) Complementary Energy Method

Consider a steel member AB subjected to axial force N and bending moment M, the complementary energy dU^* stored in the infinitesimal element dS of the member AB will be given[8] from Fig. 10, as

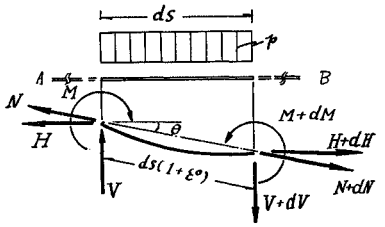

Fig. 10 Deformed Element of Member AB.

$$dU^*=\left\{\int\phi(1+\varepsilon^0)dM+\int\varepsilon^0dN-\theta\frac{dM}{dS}+(N-H)\right\}dS$$

where θ : chord slope of the element,
H : horizontal force.

Then, the total complementary energy of the member AB is

$$U^*=\iint\phi(1+\varepsilon^0)dMdS+\iint\varepsilon^0dNdS-\int\theta\frac{dM}{dS}dS+\int(N-H)dS \quad\cdots\cdots(9)$$

For the small deformation theory, Eq. (9) yields by dropping the secondary effects of the deformation.

$$U^*=\iint\phi\,dMdS+\iint\varepsilon^0dNdS \quad\cdots\cdots(10)$$

For the convenience of the analytical procedure, a sufficient number of cuts have been introduced hereupon in such a manner as to isolate each element from other elements, and the complementary energy of the member AB is expressed as the sum of the complementary energies of its individual elements.

Therefore,

$$U^*=\sum_j\int_0^\lambda\int_{M_j}\phi(1+\varepsilon_j^0)dMdS+\sum_j\int_0^\lambda\int_{N_j}\varepsilon^0dNdS-\sum_j\int_0^\lambda\theta_j\frac{dM_j}{dS}dS+\sum_j\int_0^\lambda(N_j-H_j)dS \quad\cdots\cdots(11)$$

where λ : length of element,
j : number of element, used as suffix.

On the other hand, the compatibility condtions for the i th element can be written using the complementary minimum principle[8] as

$$\frac{\partial U^*}{\partial M_i}=0 \quad\cdots\cdots(12)$$

which is transformed into

$$\sum_j\left[\int_0^\lambda\left\{\phi_j(1+\varepsilon_j^0)\frac{\partial M_j}{\partial M_i}\right\}dS-\int_0^\lambda\left\{\theta_j\frac{\partial}{\partial M_i}\left(\frac{M_{j+1}-M_j}{\lambda}\right)\right\}dS\right]=0 \quad\cdots\cdots(13)$$

or

$$\theta_i-\theta_{i-1}+\frac{\lambda}{6}\left\{2\phi_i(1+\varepsilon_i^0)+\frac{1}{2}(\phi_i+\phi_{i-1})(2+\varepsilon_i^0+\varepsilon_{i-1}^0)+\frac{1}{2}(\phi_i+\phi_{i+1})(2+\varepsilon_i^0+\varepsilon_{i+1}^0)\right\}=0 \quad\cdots\cdots(14)$$

(4) Elasto-Plastic Slope-Deflection Equation

An elasto-plastic slope-deflection equation of steel member subjected to bending moment and axial force such as shown in Fig. 11 is derived herein, for the convenience of the indeterminate structural analysis.

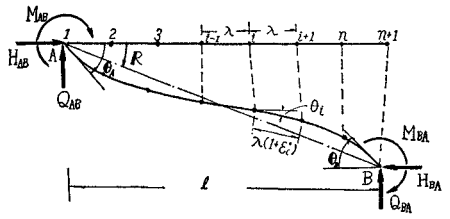

Fig. 11 Steel Member AB Subjected to End Forces M_{AB}, H_{AB}, Q_{AB} at End A and M_{BA}, H_{BA}, Q_{BA} at End B, Respectively.

Dividing the member AB into n elements, we can get moment M_i and axial force N_i at the divided point i as follows;

$$\left.\begin{aligned}M_i&=f_iM_{AB}+g_iM_{BA}+v_i^0H_{AB}+M_i^0,\\N_i&=Q_{AB}\sin\theta_i-H_{AB}\cos\theta_i\end{aligned}\right\} \quad\cdots\cdots(15)$$

where $f_i=1-u_i/u_{n+1}$, $g_i=-u_i/u_{n+1}$,
$v_i^0=v_i-v_{n+1}u_i/u_{n+1}$,
$u_i=\lambda\sum_{j=1}^{i-1}(1+\varepsilon_j^0)\cos\theta_j$,

$$v_i=\lambda\sum_{j=1}^{i-1}(1+\varepsilon_j{}^0)\sin\theta_j,$$

$$Q_{AB}=-(M_{AB}+M_{BA}+v_{n+1}H_{AB})/u_{n+1},$$

$M_i{}^0$: moment of point i due to applied loads,

M_{AB}, M_{BA} : end moments at ends A, B, respectively.

From the complementary minimum principle, rotation angles $\boldsymbol{\theta}_A$, $\boldsymbol{\theta}_B$ at ends A and B are given by using Eq. (11) as

$$\left.\begin{aligned}\boldsymbol{\theta}_A-\boldsymbol{R}&=\frac{\partial U^*}{\partial M_{AB}}=\int_A^B\phi(1+\varepsilon^0)\frac{\partial M}{\partial M_{AB}}dS\\ \boldsymbol{\theta}_B-\boldsymbol{R}&=\frac{\partial U^*}{\partial M_{BA}}=\int_A^B\phi(1+\varepsilon^0)\frac{\partial M}{\partial M_{BA}}dS\end{aligned}\right\}\quad\cdots\cdots(16)$$

where $\boldsymbol{R}$: revolution angle of member AB.

Substituting Eq. (15) into Eq. (16) and replacing ϕ by ϕ^p+M/E_0I, we get the following equation.

$$\left.\begin{aligned}E_0K(\boldsymbol{\theta}_A-\boldsymbol{R})&=a_1M_{AB}+b_1M_{BA}+C_1,\\ E_0K(\boldsymbol{\theta}_B-\boldsymbol{R})&=a_2M_{BA}+b_2M_{AB}+C_2\end{aligned}\right\}\quad\cdots(17)$$

where

$$a_1=\int_A^B f^2(1+\varepsilon^0)dS/l,$$

$$b_1=b_2=\int_A^B fg(1+\varepsilon^0)dS/l,$$

$$a_2=\int_A^B g^2(1+\varepsilon^0)dS/l,\quad \phi^p=\phi-M/E_0I,$$

$$K=I/l,\quad \bar{\phi}^p=\phi^p/\phi_y,$$

$$C_1=M_y\int_A^B f(\bar{M}^0+\bar{H}_{AB}\cdot\bar{v}^0r_0+\bar{\phi}^p)(1+\varepsilon^0)dS/l,$$

$$\bar{v}^0=v^0/l,\quad r_0=lN_y/M_y,$$

$$C_2=M_y\int_A^B g(\bar{M}^0+\bar{H}_{AB}\cdot\bar{v}^0\cdot r_0+\bar{\phi}^p)(1+\varepsilon^0)dS/l$$

$$\bar{H}_{AB}=H_{AB}/N_y,\quad \bar{M}^0=M^0/M_y$$

Thus, the required equation can be obtained by solving Eq. (17)

$$\left.\begin{aligned}M_{AB}&=E_0K(\alpha_{AB}\boldsymbol{\theta}_A+\beta_{AB}\boldsymbol{\theta}_B+\gamma_{AB}\boldsymbol{R})+C_{AB},\\ M_{BA}&=E_0K(\beta_{BA}\boldsymbol{\theta}_A+\alpha_{BA}\boldsymbol{\theta}_B+\gamma_{BA}\boldsymbol{R})+C_{BA}\end{aligned}\right\}\quad\cdots\cdots(18)$$

where $\alpha_{AB}=-a_2/a_3$, $\alpha_{BA}=-a_1/a_3$,

$\beta_{AB}=\beta_{BA}=b_1/a_3$, $a_3=b_1{}^2-a_1a_2$,

$C_{AB}=(a_2c_1-b_1c_2)/a_3$, $C_{BA}=(a_1c_2-b_2c_1)/a_3$

Eq. (18) is transformed into non-dimensional form as

$$\left.\begin{aligned}\bar{M}_{AB}&=\frac{1}{\omega}(\alpha_{AB}\boldsymbol{\theta}_A+\beta_{AB}\boldsymbol{\theta}_B+\gamma_{AB}\boldsymbol{R})+\bar{C}_{AB}\\ \bar{M}_{BA}&=\frac{1}{\omega}(\beta_{BA}\boldsymbol{\theta}_A+\alpha_{BA}\boldsymbol{\theta}_B+\gamma_{BA}\boldsymbol{R})+\bar{C}_{BA}\end{aligned}\right\}\quad\cdots\cdots(19)$$

where $\bar{C}=C/M_y$, $\omega=M_y/E_0K=\phi_yl$

(5) Illustrative Examples

a) Example-1

To illustrate this method it is applied to a cantilever AB subjected to vertical and horizontal concentrated loads at free end B.

If the cantilever is divided into 10 elements as shown in Fig. 12, equilibrium conditions will be given as follows;

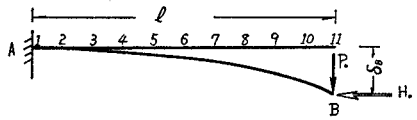

Fig. 12 Cantilever AB Subjected to Concentrated Loads H_0, P_0.

$$\left.\begin{aligned}Q_{i+1}&=P_0\cos\theta_i+H_0\sin\theta_i,\\ N_{i+1}&=P_0\sin\theta_i-H_0\cos\theta_i,\\ M_{i+1}&=M_i+Q_i(1+\varepsilon_i{}^0)\lambda,\quad(i=1\sim10)\end{aligned}\right\}\quad\cdots(20)$$

where $\theta_1=-\lambda\{\phi_1(1+\varepsilon_1{}^0)+(\phi_1+\phi_2)(2+\varepsilon_1{}^0+\varepsilon_2{}^0)/2\}/6$,

P_0 : vertical concentrated load,

H_0 : horizontal concentrated load,

Q : shearing force,

$\lambda=l/10$, l : span length,

From Eq. (20), unknown quantities M_i, N_i and Q_i will be evaluated by using trial and error method, where θ_i, ϕ_i and $\varepsilon_i{}^0$ can be determined by **Eqs. (14) and (8).**

With these quantities M_i, N_i and Q_i known, vertical displacement δ_B at the end B can be calculated by using complementary minimum principle as follows;

$$\delta_B=\frac{\partial U^*}{\partial P_0}\quad\cdots\cdots(21)$$

which yields, by utilizing Simpson's formula, as

$$\delta_B=\frac{\lambda}{3}\left(\chi_1+\chi_{11}+4\sum_{i=1}^{5}\chi_{2i}+2\sum_{i=1}^{4}\chi_{2i+1}\right)\cdots\cdots(22)$$

where

$$\chi_i=(1+\varepsilon_i{}^0)\left\{\phi_i\lambda\sum_{j=i}^{10}(1+\varepsilon_j{}^0)\cos\theta_j+\sin\theta_i-\theta_i\cos\theta_i\right\}$$

$$\chi_{11}=0$$

From the preceding investigation, relationships between applied load P_0 and deflection δ_B can be

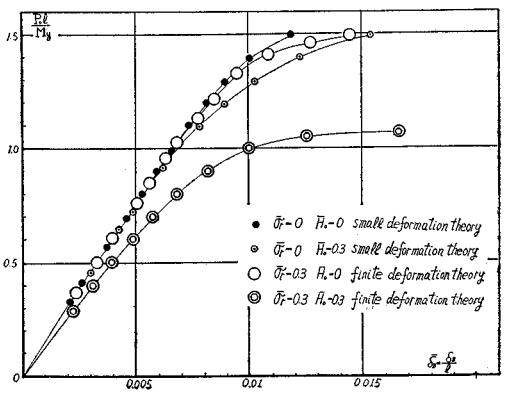

Fig. 13 Deflection Curve of the Cantilever AB with Rectangular Section under Incrementary Loading.

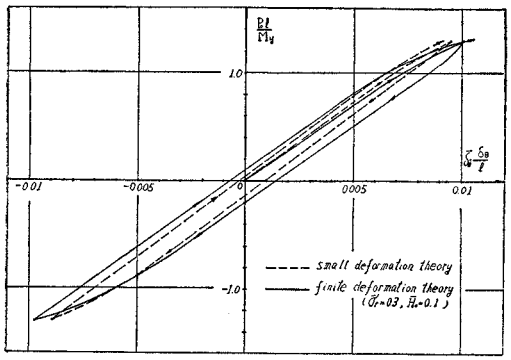

Fig. 14 Deflection Curve of the Cantilever AB with Rectangular Section under Cycric Loading.

obtained for the beam with rectangular cross section[2] by running computer program with $\Delta h=h/10$, $h=20.47$ cm, $b=2.81$ cm, $\sigma_y=2\,100$ kg/cm², $E_0=2.1\times10^6$ kg/cm², $\mu_0=0.005$, $l=10h$, $\bar{\sigma}_r=0.3$ and $\bar{H}_0$ ($=H_0/N_y$) having the value 0 and 0.3, respectively, and are plotted in Fig. 13.

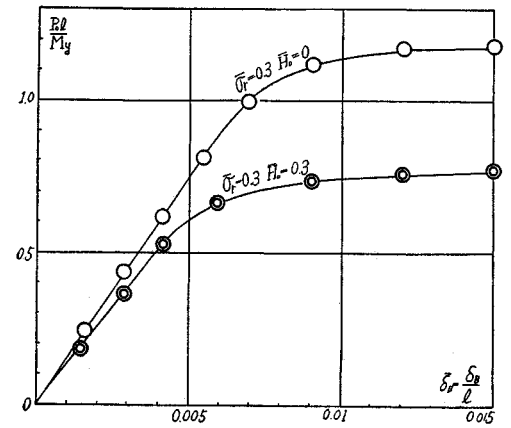

Fig. 15 Deflection Curve of the Cantilever AB with I-Section (Strong Axis) under Incrementary Loading.

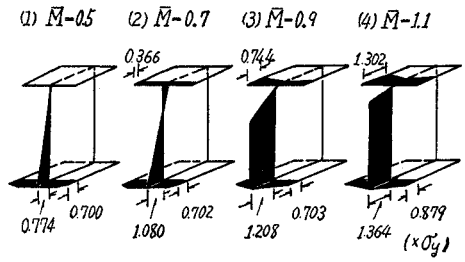

Fig. 16 Stress-Distribution Diagram for I-Section ($\bar{N}=-0,3$, $\bar{\sigma}_r=0.3$).

Comparison is made between the results of this solution and the solution given by the small deformation theory. And it is found that the bending rigidity of the beam under axial force decreases considerably by the secondary effect of the finite deformation (See Figs. 13, 14).

It is also recognized that the iteration procedure converges rapidly if initial values of the unknowns are chosen properly, and that the problem of obtaining suitably initial values of the unknowns is conveniently resolved by using the incremental load method.

Fig. 15 also shows curve for the I-section of Fig. 8.

While, the stress-distribution diagrams for the given load become as shown in Fig. 16.

b) Example-2

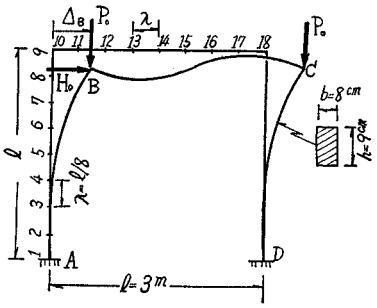

Fig. 17 Rectangular Frame Subjected Concentrated Loads H_0, P_0.

A structure of Fig. 17 is taken herein as the second example.

End moments M_{AB}, M_{BA}, M_{BC} can be expressed from the given structural and load coditions as follows;

$$\left.\begin{aligned}\bar{M}_{AB}&=\frac{1}{\omega}(\beta_{AB}\boldsymbol{\theta}_B+\gamma_{AB}\boldsymbol{R})+\bar{C}_{AB}\\ \bar{M}_{BA}&=\frac{1}{\omega}(\alpha_{BA}\boldsymbol{\theta}_B+\gamma_{BA}\boldsymbol{R})+\bar{C}_{BA}\\ \bar{M}_{BC}&=\frac{1}{\omega}(\alpha_{BC}\boldsymbol{\theta}_B+\beta_{BC}\boldsymbol{\theta}_B)+\bar{C}_{BC}\end{aligned}\right\}\cdots(23)$$

Moment equilibriun condition at joint B is

$$\bar{M}_{BA}+\bar{M}_{BC}=0 \quad\cdots\cdots(24)$$

And, force equilibrium condition is

$$\left.\begin{aligned}&\bar{H}_0-2\bar{Q}_{BA}=0,\\ &\bar{P}_0+\bar{Q}_{BC}-\bar{H}_{BA}=0\end{aligned}\right\}\cdots\cdots(25)$$

where $\bar{H}_0=H_0/N_y$, $\bar{P}_0=P_0/N_y$, $\bar{Q}=Q/N_y$, $\bar{H}=H/N_y$.

From Eqs. (23), (24) and Eq. (25), $\boldsymbol{\theta}_B$ and $\boldsymbol{R}$ will be given as

$$\boldsymbol{\theta}_B=\frac{\omega\left\{\gamma_{BA}\left(\frac{r_0}{2l}u_9\bar{H}_0+\frac{r_0}{l}v_9\bar{H}_{AB}+\bar{C}_{AB}-\bar{C}_{BC}\right)-\gamma_{AB}(\bar{C}_{BA}+\bar{C}_{BC})\right\}}{\{\gamma_{BA}(\alpha_{BC}-\beta_{AB}+\beta_{BC})+\gamma_{AB}(\alpha_{BA}+\alpha_{BC}+\beta_{BC})\}}\quad\cdots\cdots(26)$$

$$\boldsymbol{R}=\frac{1}{\gamma_{BA}}\{(\alpha_{BA}+\alpha_{BC}+\beta_{BC})\boldsymbol{\theta}_B+\omega(\bar{C}_{BA}+\bar{C}_{BC})\}$$

Then, horizontal displacement Δ_B of joint B is

$$\Delta_B = u_0 \tan \boldsymbol{R} \quad \cdots\cdots(27)$$

In the above obtained equations, chord slope θ_i ($i=2\sim8$, $11\sim17$) is defined by Eq. (12).

While, θ_1, θ_{10} are expressed by the following equations.

$$\left.\begin{aligned} &\lambda \sum_{i=10}^{17} (1+\varepsilon_i^0) \sin\theta_i = 0, \\ &\lambda \sum_{i=1}^{8} (1+\varepsilon_i^0) \sin\theta_i = \Delta_B \end{aligned}\right\}$$

or

$$\left.\begin{aligned} \theta_{10} &= \frac{1}{8}\left\{ \sum_{i=11}^{17} (18-i) J_i \right. \\ &\quad \left. - \sum_{i=10}^{17} (\varepsilon_i^0 \sin\theta_i + \sin\theta_i - \theta_i) \right\} \\ \theta_1 &= \frac{1}{8}\left\{ \sum_{i=2}^{8} (9-i) J_i \right. \\ &\quad \left. - \sum_{i=1}^{8} (\varepsilon_i^0 \sin\theta_i + \sin\theta_i - \theta_i) \right\} + \Delta_B \lambda \end{aligned}\right\} \quad \cdots\cdots(28)$$

where $J_i = \{2\phi_i(1+\varepsilon_i^0) + (\phi_i+\phi_{i-1})(2+\varepsilon_i^0+\varepsilon^0{}_{i-1})/2 + (\phi_i+\phi_{i+1})(2+\varepsilon_i^0+\varepsilon^0{}_{i+1})/2\}/6$

Using Eqs. (23), (26), (27), (28) and Eq. (8), the displacement Δ_B to the increasing loads H_0, P_0 can be calculated with the parameters of the ratio $P_0/H_0=0$ and 10.

Comparison is made in Fig. 18 between the $H_0-\Delta_B$ curves due to the finite deformation theoty and the small deformation theory.

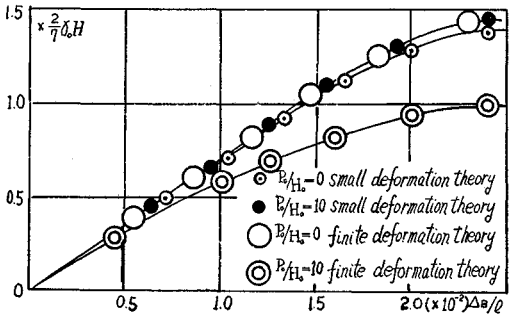

Fig. 18 Horizontal Displacement Δ_B of the Frame of Fig. 17.

4. Problem of Plastic Stability

(1) General Theory

A member AB subjected to bending moments M_{AB}, M_{BA} and horizontal force H_{AB} is shown in Fig. 19 with notation for the coordinate-axes, displacements and forces.

If the member AB is divided into n elements, moments at the every divided points of the beam are given by considering the effect of the deflection in the following matrix form.

$$[\overline{M}] = ([1]+[-\overline{X}])\cdot\overline{M}_{AB} + \overline{M}_{BA}[-\overline{X}] + \overline{H}_{AB}{}^*[\overline{Y}] + \overline{H}_{AB}{}^*\boldsymbol{R}[-\overline{X}] + [\overline{M}^0] \quad \cdots\cdots(29)$$

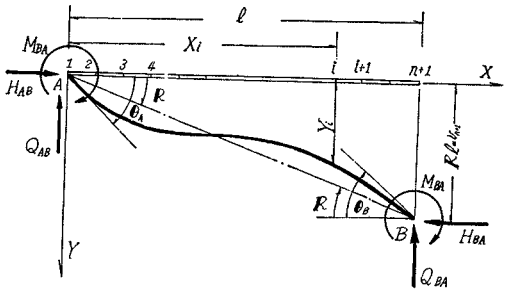

Fig. 19 Steel Member AB Subjected to M_{AB}, H_{AB}, Q_{AB} at End A and M_{BA}, H_{BA}, Q_{BA} at End B.

where

$$[\overline{M}] = \begin{bmatrix} \overline{M}_1 \\ \overline{M}_2 \\ \vdots \\ \overline{M}_n \end{bmatrix}, \quad [1] = \begin{bmatrix} 1 \\ 1 \\ \vdots \\ 1 \end{bmatrix},$$

$$[-\overline{X}] = \begin{bmatrix} -\overline{X}_1 \\ -\overline{X}_2 \\ \vdots \\ -\overline{X}_n \end{bmatrix}, \quad [\overline{Y}] = \begin{bmatrix} \overline{Y}_1 \\ \overline{Y}_2 \\ \vdots \\ \overline{Y}_n \end{bmatrix},$$

$$[\overline{M}^0] = \begin{bmatrix} \overline{M}^0{}_1 \\ \overline{M}^0{}_2 \\ \vdots \\ \overline{M}^0{}_n \end{bmatrix},$$

$\overline{X}_i = X_i/l$, $\overline{Y}_i = Y_i/l$,

$\overline{H}_{AB}{}^* = r_0 \overline{H}_{AB}$

Y_i : vertical displacement at point i.

Then, rotation angles $\boldsymbol{\theta}_A$, $\boldsymbol{\theta}_B$ at both ends are given from Eq. (10) as follows ;

$$\left.\begin{aligned} \boldsymbol{\theta}_A - \boldsymbol{R} &= \frac{\partial U^*}{\partial M_{AB}} = \omega \int_A^B \bar{\phi}(1-\overline{X})\, d\overline{X} \\ \boldsymbol{\theta}_B - \boldsymbol{R} &= \frac{\partial U^*}{\partial M_{BA}} = \omega \int_A^B \bar{\phi}(-\overline{X})\, d\overline{X} \end{aligned}\right\} \cdots(30)$$

which can be rewritten in the following matrix form.

$$\left.\begin{aligned} \boldsymbol{\theta}_A - \boldsymbol{R} &= \omega([a][\bar{\phi}] + a_B \bar{\phi}_B) \\ \boldsymbol{\theta}_B - \boldsymbol{R} &= \omega([b][\bar{\phi}] + b_B \bar{\phi}_B) \end{aligned}\right\} \quad \cdots\cdots(31)$$

where $[a]$, $[b]$: raw matrix of order $(1, n)$,

$[\bar{\phi}]$: column matrix of order $(n, 1)$,

$\bar{\phi}_B$: curvature at the end B.

The vertical displacement Y_i at point i can be obtained from the formula of ϕ-Method[4] as follows (See Fig. 20) ;

$$Y_i = X_i \boldsymbol{\theta}_A - \int_0^{X_i} \phi(X_i - X)\, dX, \quad (i=1, 2, \cdots n) \quad \cdots\cdots(32)$$

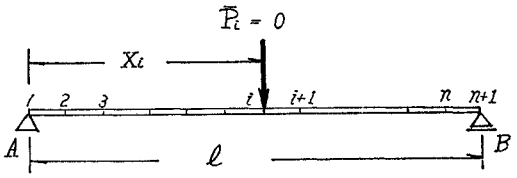

Fig. 20 Simple Beam AB Subjected to Virtual Concentrated Load $\overline{P}_i=0$ at Point i.

In general, the above obtained equation can be transformed into the following matrix form,

$$[\bar{Y}]=\boldsymbol{\theta}_A[\bar{X}]-\omega([\alpha][\bar{\phi}]+[\beta]\cdot\bar{\phi}_B) \quad \cdots\cdots(33)$$

where $[\alpha]$: square matrix of order (n, n),

$[\beta]$: column matrix of order $(n, 1)$.

On the other hand, the curvature at point i is generally rewritten from Fq. (8) as,

$$\bar{\phi}_i=\bar{M}_i+\xi_i,\ (i=1, 2, \cdots n, B),$$

where $\xi_i=\bar{\phi}_i-\bar{M}_i$

which yields

$$[\bar{\phi}]=[\bar{M}]+[\xi] \quad \cdots\cdots(34)$$

and $$\bar{\phi}_B=-\bar{M}_{BA}+\xi_B \quad \cdots\cdots(35)$$

where $[\xi]$: column matrix of order $(n, 1)$ with respect to ξ_i.

Substituting Eq. (29) into Eq. (34), we have

$$\begin{aligned}[\bar{\phi}]=&\bar{M}_{AB}([1]+[-\bar{X}])\\&+\bar{M}_{BA}\cdot[-\bar{X}]+\bar{H}_{AB}{}^*[\bar{Y}]\\&+\bar{H}_{AB}{}^*\boldsymbol{R}[-\bar{X}]+[\bar{M}^0]+[\xi]\end{aligned} \quad \cdots\cdots(36)$$

Substituting Eq. (33) into Eq. (36), we have

$$\begin{aligned}&\{[I]+\omega\bar{H}_{AB}{}^*\cdot[\alpha]\}[\bar{\phi}]\\&=\bar{M}_{AB}([1]+[-\bar{X}])\\&\quad+\bar{M}_{BA}[-\bar{X}]-\bar{H}_{AB}{}^*(\boldsymbol{\theta}_A-\boldsymbol{R})\\&\quad\cdot[-\bar{X}]-\omega\bar{H}_{AB}{}^*\bar{\phi}_B\cdot[\beta]\\&\quad+[\bar{M}^0]+[\xi]\end{aligned}$$

which is transformed into

$$\begin{aligned}[\bar{\phi}]=&\bar{M}_{AB}\cdot([1^*]+[X^*])+\bar{M}_{BA}\cdot[X^*]\\&-\bar{H}_{AB}{}^*(\boldsymbol{\theta}_A-\boldsymbol{R})\cdot[X^*]\\&-\omega\bar{H}_{AB}{}^*\bar{\phi}_B\cdot[\beta^*]+[M^*]+[\xi^*]\end{aligned} \cdots(37)$$

where $[1^*]=[\zeta]^{-1}[1]$, $[X^*]=[\zeta]^{-1}[-\bar{X}]$,

$[\beta^*]=[\zeta]^{-1}[\beta]$, $[M^*]=[\zeta]^{-1}[\bar{M}^0]$,

$[\xi^*]=[\zeta]^{-1}[\xi]$,

$[I]$: unit matrix of the n th order,

$[\zeta]=[I]+\omega\bar{H}_{AB}{}^*\cdot[\alpha]$

From, Eqs. (31), (36) and (37), we have

$$\begin{aligned}&(1+\omega\bar{H}_{AB}{}^*[a][X^*])(\boldsymbol{\theta}_A-\boldsymbol{R})\\&=\omega\{\bar{M}_{AB}\cdot[a]([1^*]+[X^*])\\&\quad+\bar{M}_{BA}([a][X^*]-\beta_a)\\&\quad+[a]([M^*]+[\xi^*])+\beta_a\xi_B\},\end{aligned} \cdots\cdots(38)$$

$$\begin{aligned}&\omega\bar{H}^*{}_{AB}[b][X^*]\cdot\boldsymbol{\theta}_A+\boldsymbol{\theta}_B\\&\quad-(1+\omega\bar{H}_{AB}{}^*[b][X^*])\boldsymbol{R}\\&=\omega\{\bar{M}_{AB}[b]([1^*]+[X^*])\\&\quad+\bar{M}_{BA}([b][X^*]-\beta_b)\\&\quad+[b]([M^*]+[\xi^*])+\beta_b\xi_B\}\end{aligned} \cdots\cdots(39)$$

where $\beta_a=a_B-\omega\bar{H}_{AB}{}^*[a][\beta^*]$,

$\beta_b=b_B-\omega\bar{H}_{AB}{}^*[b][\beta^*]$

Eqs. (38) and (39) are rewritten in the following matrix form.

$$[\boldsymbol{A}]\begin{bmatrix}\bar{M}_{AB}\\ \bar{M}_{BA}\end{bmatrix}=\frac{1}{\omega}[\boldsymbol{B}]\begin{bmatrix}\boldsymbol{\theta}_A\\ \boldsymbol{\theta}_B\\ \boldsymbol{R}\end{bmatrix}+[\boldsymbol{C}] \quad \cdots\cdots(40)$$

Finally, we can get the required formula as

$$\begin{bmatrix}\bar{M}_{AB}\\ \bar{M}_{BA}\end{bmatrix}=\frac{1}{\omega}[\boldsymbol{K}]\begin{bmatrix}\boldsymbol{\theta}_A\\ \boldsymbol{\theta}_B\\ \boldsymbol{R}\end{bmatrix}+[\overline{\boldsymbol{M}}] \quad \cdots\cdots(41)$$

where $[\boldsymbol{K}]=[\boldsymbol{A}]^{-1}[\boldsymbol{B}]$, $[\overline{\boldsymbol{M}}]=[\boldsymbol{A}]^{-1}[\boldsymbol{C}]$,

$$[\boldsymbol{A}]=\begin{bmatrix}[a][1^*]+[a][X^*] & [a][X^*]-\beta_a\\ [b][1^*]+[b][X^*] & [b][X^*]-\beta_b\end{bmatrix}$$

$$[\boldsymbol{B}]=\begin{bmatrix}(1+\omega\bar{H}_{AB}{}^*[a][X^*]) & 0\\ & -(1+\omega\bar{H}_{AB}{}^*[a][X^*])\\ (0+\omega\bar{H}_{AB}{}^*[n][X^*]) & 1\\ & -(1+\omega\bar{H}_{AB}{}^*[b][X^*])\end{bmatrix}$$

$$[\boldsymbol{C}]=\begin{bmatrix}[a][M^*]+[a][\xi^*]+\beta_a\xi_B\\ [b][M^*]+[b][\xi^*]+\beta_b\xi_B\end{bmatrix}$$

(2) Illustrative Example

A cantilever with H-section of Fig. 21 is considered herein for the demonstration of this method.

From Fig. 21, end moments M_{AB}, M_{BA} and M^0 are given as

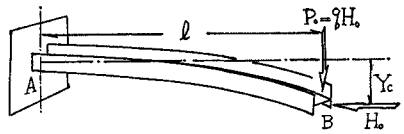

Fig. 21 Cantilever AB Subjected to Concentrated Loads H_0, P_0 $(=H_0)$.

$$\left.\begin{aligned}&\bar{M}_{AB}=-\bar{H}_0{}^*q-\bar{H}_0{}^*\bar{Y}_C\\&\bar{M}_{BA}=0,\\&\bar{M}^0=0.\end{aligned}\right\} \cdots\cdots(42)$$

And Eq. (38) can be rewritten by putting $\boldsymbol{R}=\bar{Y}_C$, $\bar{H}_{AB}{}^*=\bar{H}_0{}^*$ as

$$\begin{aligned}&(1+\omega\bar{H}_0{}^*[a][X^*])(\boldsymbol{\theta}_A-\bar{Y}_c)\\&\quad=\omega\{\bar{M}_{AB}[a]([1^*]+[X^*])\\&\qquad+\bar{M}_{BA}([a][X^*]-\beta_a)\\&\qquad+[a]([M^*]+[\xi^*]+\beta_a\xi_B\}\end{aligned} \cdots\cdots(43)$$

Substituting Eq. (42) into Eq. (43), we have

$$\begin{aligned}&(1+\omega\bar{H}_0{}^*[a][X^*])(\boldsymbol{\theta}_A-\bar{Y}_c)\\&\quad=\omega\{-\bar{H}_0{}^*q[a]([1^*]+[X^*])\\&\qquad-\bar{H}_0{}^*\bar{Y}_c[a]([1^*]+[X^*])\\&\qquad+[a][\xi^*]+\beta_a\xi_B\}\end{aligned} \cdots\cdots(44)$$

By using boundary conditions $\boldsymbol{\theta}_A=0$, $\xi_B=0$ ($\because$ $M_{BA}=0$), we can finally get the required equation from Eq. (44) as follows;

$$q=\frac{(1-\omega\bar{H}_0{}^*[a][1^*])\bar{Y}_c+\omega[a][\xi^*]}{\omega\bar{H}_0{}^*[a]([1^*]+[X^*])} \quad \cdots(45)$$

where $[a]=\frac{\bar{\lambda}^2}{6}\cdot[3n-1\ \ 6(n-1)\ \ 6(n-2)\cdots 12\ \ 6]$,

$$[-\bar{X}]=\begin{bmatrix}0\\ -1/n\\ -2/n\\ \vdots\\ -(n-1)/n\end{bmatrix}$$

$$[\alpha]=\frac{\bar{\lambda}^2}{6}\cdot\begin{bmatrix}0 & 0 & 0 & 0\cdots\cdots 0\\ 2 & 1 & 0 & 0\cdots\cdots 0\\ 5 & 6 & 1 & 0\cdots\cdots 0\\ 8 & 12 & 6 & 1\cdots\cdots 0\\ \vdots & \vdots & \vdots & \ddots\ \ \vdots\\ 3(n-2)-1 & 6(n-3) & 6(n-4) & \ddots\ \ \vdots\\ 3(n-1)-1 & 6(n-2) & 6(n-3) & \cdots\cdots 1\end{bmatrix}$$

From the foregoing investigation, $q-\bar{Y}_c$ curve can be obtained for the H-section including residual

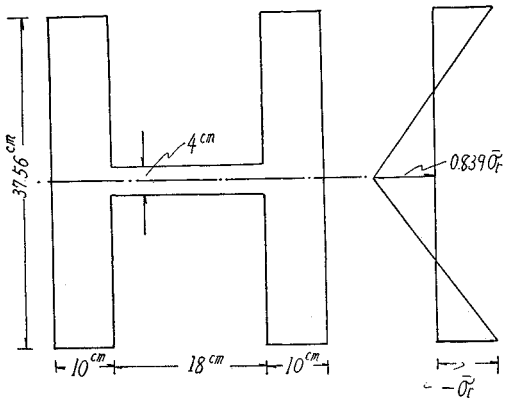

Fig. 22 Residual Stress-Distribution Diagram for H-Section.

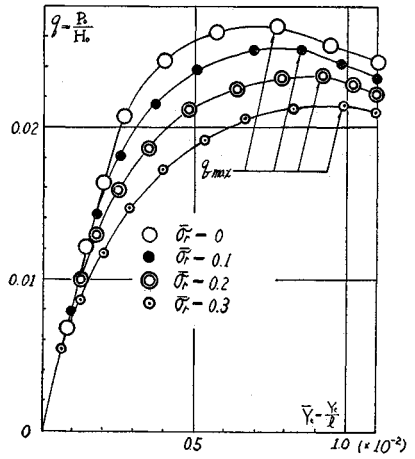

Fig. 23 q-$\bar{Y}_c$ Curve of the Cantilever AB Subjected to Weak-Axis Bending Combined with Axial Thrust.

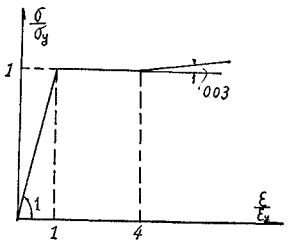

Fig. 24 Stress-Strain Curve.

stress, shown in Fig. 22, by running computer program with $\bar{H}_0=0.7$, $\mu_0=0.001$, $\Delta\bar{h}=0.1$, $h=37.56$ cm, $t=10$ cm, $w=4$ cm, $l=170$ cm, $\sigma_y=3\,300$ kg/cm^2, $E_0=2.1\times10^6$ kg/cm^2 and $\bar{\sigma}_r$ having the values 0, 0.1, 0.2, 0.3, respectively, and protted in Fig. 23, where the effect of the stress in the web is disregarded.

The transition points from stable to unstable equilibrium in Fig. 23 are given in Table 2. In the case of $\bar{\sigma}_r=0$, the above obtained values (0.0270, 0.765×10^{-2}) are good agreement with the ones[10]

Table 2 Transition Points from Stable to Unstable Equilibrium.

$\bar{\sigma}_r$	$q_{max}=q_c$	$\bar{Y}_c$
0	0.0270	0.765×10^{-2}
0.1	0.0252	0.838 〃
0.2	0.0235	0.919 〃
0.3	0.0217	0.978 〃

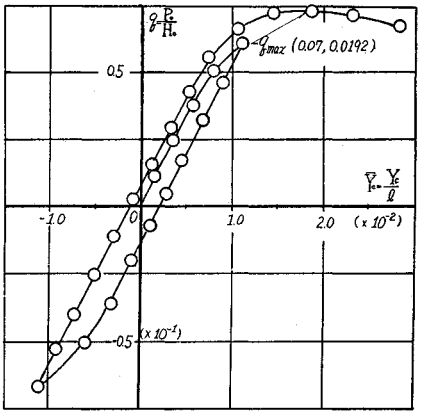

Fig. 25 q-$\bar{Y}_c$ Curve of the Cantilever of Fig. 21 with Rectangular Section under Repeated Loading.

(0.0286, 0.765×10^{-2}) estimated by using the stress-strain curve of Fig. 24. Fig. 25 is cycric load-deflection curve diagram of same cantilever beam with $\bar{H}_0=0.3$, $\mu_0=0.5$, $\Delta\bar{h}=0.1$, $h=37.56$ cm, $b=20$ cm, $l=170$ cm, $\sigma_y=2\,400$ kg/cm^2, $E_0=2.1\times10^6$ kg/cm^2 and $\bar{\sigma}_r=0$.

5. Conclusion

In this paper, the authors have suceeded in deriving general formula for the curvature of steel member subjected to bending moment combined with axial force, based on the numerical integration technique and interation method.

The derived formula is then used to analyze elasto-plastic finite deformations of steel structures and to determine the critical loads employing the extended complementary energy method, wherein the effect of residual stress can be taken into account.

The iteration procedure, as presented, converges rapidly for any variable load by utilizing the incremental load method.

By the way, if a steel member is subjected to axial force in addition to bending moment, it is reasonable to expect that the rigidity of the member is influenced by the residual stress and finite deformation.

This fact is clarified in Examples of Fig. 12, Fig. 17 and Fig. 21 in which the deflection increases

remarkably by the effect of the residual stress or that of the finite deformation.

Although these numerical examples deal with such simple structures as cantilever or rectangular frame of Fig. 17, the presented method is, of course, applicable to more complicated structures.

Thus, it may be concluded that the advantages of this method are its simplicity and generality of formnlation, and even its applicability to a great variety of problems with complicated loading and structural conditions.

REFERENCES

1) K.E. Knudsen, C.H. Yang, W.H. Weiskopf, et al.: Plastic Strength and Deflections of Continuous Beams, Progress Report, No. 9, The Welding Journal, Vol. 32, May 1953.
2) R.L. Ketter, E.L. Kaminsky and L.S. Beedle : Plastic Defomation of Wide-Flange Beam-Columns, Trans of the A.S.C.E., Vol. 120, 1955.
3) K.H. Gerstle and V. Zarboulas : Elastic-Plastic Deformations of Steel Structures, Proc. of the A.S.C.E., Vol. 89, ST 1, Feb. 1963.
4) T. Yamasaki, T. Ohta and N. Ishikawa : Elastoc-Plastic Analysis of Frames By Complementary Energy Method, Proc. of the J.S.C.E., No. 134, Oct. 1966.
5) T. Yamasaki, T. Ohta : Simplified Elasto-Plastic Analysis of Structures by Complementary Energy Method, Proc. of the Fifteenth J.N.C. for A.M., 1965, Decem. 1966.
6) T. Yamasaki, T. Ohta, N. Ishikawa and H. Matsuguma : The Study on the Elasto-Plastic Analysis of Steel Frames under Variable Repeated Loading, Technology Reports of the Kyushu University, Vol. 42, No. 3, June 1969.
7) S. Igarashi, C. Matsui, K. Koshimura and K. Matsumura : Inelastic Behaviors of Structural Steel Section under Alternative Loadings, (1) Method of Anlysis and Example, Trans of the A.I.J., No. 169, March, 1970.
8) C. Oran : Complementary Energy Concept for Large Deformation, Jour. of the S.D., Proc. of the A.S.C.E., ST 1, Feb. 1967.
9) K. Horii and M. Kawahara : Elastic-Plastic Analysis of Plane Frameworks with Large Deformations. Proc. of J.S.C.E., No. 169, Sept. 1969.
10) J. Sakamoto and T. Miyamura : Elsto-Plastic Behavior of Steel Frames (Part II), Trans. of the Architectural Institute of Japan, No. 113, July 1965.

(Received Dec. 3, 1970)